Dornan T, Fielding S, Saunders RA, Genner MJ. 2021 Large mesopelagic fish biomass in the Southern Ocean resolved by acoustic properties. *Proc. R. Soc. B.* (doi: 10.1098/rspb.2021.1781)

Electronic supplementary material

PDF file includes:

Supplementary text

Figures S1 to S6

Tables S1 to S11

SI References

Electronic supplementary material

Here we provide additional detail on methodology and results for modelling fish biomass for the Southern Ocean from active acoustic data. First we describe the models for estimating target strength for Scotia Sea mesopelagic fish. Table S2 gives an overview of the source of morphological parameters for each of the mesopelagic fish taxa included in the study. We then describe acoustic backscatter modelling using generalised additive mixed models (GAMM) in relation to environmental predictors for the Southern Ocean, and the conversion of predicted backscatter (Nautical Area Scattering Coefficient, m^2 nm^{-2}) to fish biomass, including sensitivity analyses into the effect of altering fish target strength and adding Antarctic krill (*Euphausia superba*) into the model.

Modelling fish target strength (TS)

Overview

We modelled the TS (dB re 1 m^2) for eleven of the most abundant mesopelagic fish taxa, that collectively account for >94% of mesopelagic fish by abundance in rectangular mid-water trawl (RMT25) net samples [1], parameterized using locally derived fish morphometry and seawater metrics.

Finite cylinder model – Non-gas bearing fish

For fish lacking a gas-filled swimbladder [1], a fixed finite cylinder model was used to calculate TS following Stanton *et al*. [2], equations S1-S9, with slight modifications to annotation. The model, which was originally developed for zooplankton, considers cylinder tapering, is independent of the degree of curvature, and is effective on a range of angles of orientation. Whilst the model is limited when the acoustic wavelength is much smaller than the cross sectional radius of the object being modelled (in this case half the width of the fish body), this was negligible as a 38 kHz frequency wave has a wavelength of ~39.5 mm in seawater and the micronekton, the focus of this study, are typically small animals. Target strength was calculated as:

$$TS = 10\ \log_{10}(\sigma_{bs}) \qquad \text{Eq. S1}$$

$$\sigma_{bs} = A_{ij}\mathcal{R}_{12}^2\langle|I_0|^2\rangle_L \beta^{-1}\bar{L}^2 \qquad \text{Eq. S2}$$

$$\langle|I_0|^2\rangle_L = 2\{1 - exp[-8(k\bar{a}s)^2]\cos(4k\bar{a} + \mu_{p=2})\} \qquad \text{Eq. S3}$$

$$\beta = \frac{L}{a} \qquad \text{Eq. S4}$$

$$k = \frac{2\pi f}{c_{sw}} \qquad \text{Eq. S5}$$

$$s = \frac{sL}{\bar{L}} \qquad \text{Eq. S6}$$

$$\mathcal{R}_{1,2} = \frac{g\times h-1}{g\times h+1} \qquad \text{Eq. S7}$$

$$g = \frac{\rho_f}{\rho_{sw}} \qquad \text{Eq. S8}$$

$$h = \frac{c_f}{c_{sw}} \qquad \text{Eq. S9}$$

Where, σ_{bs} is the acoustic backscattering cross-section in m^2, k is wave number, f is acoustic frequency in Hz. The reflection coefficient $\mathcal{R}_{1,2}$ is the plane wave/plane interface reflection coefficient between seawater and fish tissue. g is density contrast between fish tissue density and seawater density, where ρ_{sw} and ρ_f are density of seawater and fish tissue in g ml^{-1} respectively, h is sound speed contrast between fish and seawater, c_{sw} and c_f are sound speed ms^{-1} in seawater and fish respectively.

sL is the standard deviation of fish length, L and $\bar{L}$ is standard length and mean standard length of fish, a and $\bar{a}$ are the cross sectional and mean cross sectional radius i.e. half of fish body width. Length-width ratios were used to calculate radius a from fish length. Constant values were used for A_{ij} = 0.08, sound speed of fish tissue c_f= 1510 ms^{-1} based on measured c_f for the myctophid *Stenobrachius leucopsarus* at 4 °C [3], s is the relative standard deviation of length (standard deviation of length/length) and was set at 0.1 to minimize nulls [2]. Density of seawater ρ_{sw} (1.0274 g ml^{-1}) and speed of sound in seawater c_{sw} (1465.836 ms^{-1}) were estimated from conductivity temperature depth (CTD) profile data from the same cruise (JR16003) as the density experiment (tables S3 and S4).

Prolate spheroid model – Gas bearing fish

A prolate spheroid scattering model [4-6] was used to calculate TS at 38 kHz for the equivalent spherical radius (ESR) of the gas component of the fishes swimbladder, for each of the five gas-bearing mesopelagic fish species: *Electrona carlsbergi*, small *Electrona antarctica* (< 51.378 mm), *Krefftichthys anderssoni*, *Protomyctophum bolini* and *Protomyctophum tenisoni*. Target strength was calculated using equations S10-S14 from Kloser *et al*. [6]:

$$\mathrm{TS} = 10\log_{10}(\sigma_{bs}) \qquad \text{Eq. S10}$$

$$\sigma_{bs} = {a_{es}}^2\left(\left(\left(\frac{f_p}{f}\right)^2 - 1\right)^2 + \frac{1}{Q^2}\right)^{-1} \qquad \text{Eq. S11}$$

$$f_p = f_o\, 2^{\frac{1}{2}}\, e^{-\frac{1}{3}}\,(1-e^2)^{\frac{1}{4}}\left\{ln\left(\frac{1+(1-e^2)^{\frac{1}{2}}}{1-(1-e^2)^{\frac{1}{2}}}\right)\right\}^{-\frac{1}{2}} \qquad \text{Eq. S12}$$

$$f_o = \frac{1}{2\pi a_{es}}\left(\frac{3\gamma P+4\mu_1}{\rho_f}\right)^{\frac{1}{2}} \qquad \text{Eq. S13}$$

$$P = (1 + 0.103D)10^5 \qquad \text{Eq. S14}$$

Where, σ_{bs} is the acoustic backscattering cross section in m^2 and a_{es} is the equivalent spherical radius of gas volume in m. f is acoustic frequency in Hz, f_p and f_o prolate and spherical resonant frequencies respectively, P is hydrostatic pressure in Pascals at fish depth D in metres, ρ_f is fish tissue density in kg m^{-3}. Prolate spheroid roundness e, is the ratio between minor semi-axis and major semi-axis of gas bubble, this was fixed at 0.3 based on measurements (n = 4) from computed tomography scans of *Krefftichthys anderssoni* [1].

Assumed values were used for resonance quality factor $Q = 5$; the real part of the complex shear modulus of fish tissue $\mu_1 = 10^5$ Pa; and the ratio of specific heats for swimbladder gas $\gamma = 1.4$ [5, 6].

Resonance

Resonance is a depth related phenomenon that results in a disproportionately high level of backscatter, resulting from a soundwave encountering a swimbladder diameter approximately equal to the insonifying wavelength. To assess potential for resonance bias, we modelled the theoretical relative frequency responses for a range of swimbladder radii (0.2-4 mm), following Kloser et al. [6]. Above an equivalent spherical radius of 1 mm, the effect of resonance throughout the surface to 1000 m depth range was limited (see figure S1). As the gas equivalent spherical radius of all of the gas-bearing species in this study was greater than 1 mm, the effect of resonance was not modelled within TS and biomass estimates.

Acoustic modelling – GAMM

Candidate environmental predictors of backscatter

Environmental predictors of acoustic backscatter (NASC, m^2 nmi^{-2}) considered were sea surface temperature (SST), sea temperature at 200 m (ST_{200}), net primary productivity (NPP), geopotential height as a proxy for the location of fronts and water masses, geostrophic current speed, maximum sea ice cover (percentage) preceding the acoustic sample date, water depth (bathymetry), and daylight hours (the hours between sunrise and sunset). Binomial factors included ‘day’ or ‘night’, and ‘sea ice zone’, which was classified as ‘sea ice’ when the maximum percentage sea ice concentration ≥ 15%. Regions of high productivity were characterised using a mean climatology of NPP covering summer months of the study period (Jan-Mar 2005-2017 inclusive). All other environmental data was extracted corresponding to the same date that the acoustic sample was collected or the nearest prior date (for weekly or monthly climatologies), by latitude and longitude. Environmental datasets and their sources are summarised in table S7.

All environmental raster data was in WGS84 projection with the exception of sea ice and net primary productivity data, which were re-projected from Antarctic Polar Stereographic and Equidistant Cylindrical respectively to WGS84 using the R ‘raster’ package [7]. Based on exploratory density plots, net primary productivity and response variable NASC were both $\log_e$ transformed, and geostrophic current was square root transformed prior to GAMM fitting, to downweight extreme values.

Prior to fitting the GAMM environmental predictor variables were assessed for collinearity using pairwise plots, Pearson correlation coefficients and Variance Inflation Factors (VIF). Where collinearity was identified variables were eliminated to reduce the possibility of Type II errors [8]. As geopotential height, ST_{200} and SST were all highly correlated to each other, only SST was retained for modelling, as it was the most highly correlated with NASC (figure S2). Variables with VIF > 3 were dropped sequentially until all VIF < 3, resulting in the removal of binomial variable sea ice zone [8].

The final full candidate model selection included smoothing terms for SST (sea surface temperature °C), Depth (water depth m), NPP ($\log_e$ of net primary productivity mg C m^{-2} d^{-1}), CurrSpeed (square root of geostrophic current speed ms^{-1}), DHr (Daylight hours), SIP (maximum percentage sea ice cover %); and binomial term DN (Day or Night). Using R package 'mgcv' [9] scaled t family GAMMs were fitted using a Restricted Maximum Likelihood (REML), and penalised thin plate regression splines used on all smooth terms with a conservative value of k = 3 to constrain overfitting.

The full candidate model specification was:

$$\log_e NASC \sim s(NPP, k = 3) + s(CurrSpeed, k = 3) + s(SST, k = 3) + s(Depth, k = 3) \\ + s(DHr, k = 3) + s(SIP, k = 3) + DN$$

Spatial autocorrelation

Regularly spaced acoustic data is likely to exhibit a degree of spatial autocorrelation, resulting in a violation of the assumption of independence between samples [8, 10]. To test for spatial autocorrelation Moran's I was calculated on model residuals using R package 'ape' [11], and an autoregressive correlation structure of order 1 (corAR1) was subsequently specified in GAMMs [12].

Model selection

Once the model was built variables were dropped sequentially from the full model to evaluate their relative importance for explaining deviance in acoustic backscatter. ΔAIC, BIC and adjusted R^2 values were used to identify the most parsimonious model.

Final model used to predict $\log_e$ NASC:

```
Final_model <- gamm(logNASC ~ s(lognpp, k = 3) + s(sqrt_current_ms, k = 3) +
s(sst_centigrade, k = 3) + + s(hours_light, k = 3) + s(MaxSeaIce_Perc, k = 3)
                family = "scat",
                method = "REML",
                data=twc,
                na.action="na.fail",
                correlation = corAR1(form=~Interval | cruise_id))
```

Where $\log_e$NASC is the Scotia Sea $\log_e$ transformed NASC variable in 1 km distance sampling units. "scat" is "scaled t" family, "Interval" is a numeric value that sequentially identifies each 1 km distance (1, 2, 3…i), and cruise a unique cruise leg identifier, i.e. autocorrelation structure is fitted sequentially within each cruise leg. "twc" is the echo integrated Scotia Sea total water column NASC data set, restricted to data where the water depth was ≥1000 m.

The full GAMM explained 58.3% of the variance in Scotia Sea acoustic backscatter data. F statistics clearly reveal that the major contributors to explaining NASC variability were sea surface temperature (F = 316.89), followed by daylight hours (F = 153.66) and maximum percentage sea ice (F = 97.40). Sequentially dropping environmental predictors from the GAMM enabled the selection a parsimonious model with smoothing terms for SST, NPP, CurrSpeed, DHr and SIP (figure S3), which still explained 57.9% of the variance and had a ΔAIC score <10, lowest BIC score in comparison with the full model specification (table S8).

On checking the GAMM fit, model residuals broadly conformed to normality (figure S4), with a small number of outlying points. While the vast majority of residuals were normally distributed and NASC values reasonably predicted by the model, a limited number are likely to be overestimated.

From predicted NASC to biomass

A schematic summarising the data processing flow, from net samples and environmental data to biomass estimation, is shown in figure S5.

Predicting NASC

We predicted $\log_e$ NASC for the Southern Ocean using the reduced GAMM, and the gam.predict function in R package 'mgcv' [9]. The model was parameterised with environmental climatologies of SST [13], NPP [14], Geostrophic current speed [15-17], daylight hours [18], and sea ice concentration [19] (figure S6). All $\log_e$ NASC values were converted back to the linear domain prior to abundance calculations.

Assigning species proportions

The proportions of fish species across the region were assigned based on the relative proportions of each taxa found in stratified night-time RMT25 net samples (table S5) and common SST values throughout the region. Using R package 'raster' [7], each net sample was allocated into a 1 °C SST 'group', based on the SST in the environmental climatology at each net sample location. Mean species abundance was then calculated for each of the 1 °C SST groups (table S9). Each 0.25° grid cell was assigned a proportional fish community composition, on the basis of the SST at that grid cell.

NASC to abundance

The proportional contribution of each species to the acoustic signal (NASC) was calculated for each cell using the abundance of species and the species-specific TS models, using equations in [20, 21] with slight modification to annotation. Where the TS of each species *i* was converted into the linear domain i.e. the backscattering cross-section (σ_{bs}) of species *i*:

$$\sigma_{bs_i} = 10^{TS_i/10} \qquad \text{Eq. S15}$$

Backscatter from multiple individuals within each species was found by multiplying backscattering cross section of each species by mean species abundance *N*:

$$N_i \times \sigma_{bs_i} \qquad \text{Eq. S16}$$

Proportion *P* of fish species *i* contribution to backscatter is calculated by dividing total linear backscatter of species *i* by total linear backscatter of all species, where *n* is the number of fish species:

$$P_i = \frac{N_i \times \sigma_{bs_i}}{\sum_{i=1}^{n} N_i \times \sigma_{bs_i}} \qquad \text{Eq. S17}$$

Abundance (ρ_a ind. m^{-2}) of species *i* is obtained by multiplying NASC by proportion of species *i* contribution to backscatter, then dividing by the backscattering cross-section of species *i*.

$$\rho_{a_i} = \frac{NASC \times P_i}{\sigma_{bs_i} \times 4 \times \pi \times 1852^2} \qquad \text{Eq. S18}$$

Once fish abundance was calculated from NASC, the biomass of each species in g m^{-2} was calculated by multiplying each predicted species abundance by the wet weight of a median length fish, calculated from length weight regressions (table S6).

To obtain total Scotia Sea and Southern Ocean biomass estimates, each 0.25° biomass estimate (g m^{-2}), was multiplied by the area of the 0.25° resolution cell using R package ‘raster’ [7], and all cell values within the Scotia Sea or Southern Ocean region were summed, excluding no data cells.

Sensitivity analyses

To quantify variability in biomass estimates, we ran 2000 random permutations without replacement, allowing the TS of each fish taxa to vary between its median, 25th and 75th percentiles of TS, assuming that fish were responsible for all of the acoustic backscatter (table S10).

Since fish are not the only contributors to acoustic backscatter, Antarctic krill was incorporated into the model, to assess the effect on fish biomass estimates. Individual krill are relatively weak sound scatterers at 38 kHz, however, their abundance and swarming behaviour can make them ‘visible’ in the acoustic signal. Krill length frequencies from cruises JR161, JR177 and JR200 were extracted from *Krillbase* [22] and used to calculate the median length krill in the Scotia Sea (45.00 mm). Median krill TS of -79.90 dB re 1 m^2, was derived using the stochastic distorted wave borne approximation (SDWBA) TS model, parameterised for orientation, speed of sound and density contrast [23-25].

Krill abundance (ρ_a krill. m^{-2}) estimates were taken from literature, and applied at a value of 64 krill m^{-2} throughout the Southern Ocean [26], and their influence tested by halving and doubling this value. As final krill abundance per unit area was estimated from literature, it was necessary to reduce the proportion of backscatter attributable to fish in the model. The theoretical number of krill in a net N_{krill} was back calculated using equations S19-S20:

$$P_{krill} = \frac{\rho_{a_{krill}} \times \sigma_{bs_k} \times 4 \times \pi \times 1852^2}{NASC} \qquad \text{Eq. S19}$$

$$N_{krill} = \frac{P_{krill} \times \sum_{i=1}^{n} N_i \times \sigma_{bs_i}}{\sigma_{bs_{krill}} - \left(\sigma_{bs_{krill}} \times P_{krill}\right)} \qquad \text{Eq. S20}$$

Allowing fish TS to vary, we ran 2000 random permutations without replacement for each of the krill scenarios i.e. assuming that krill contributed to backscatter at rates of 64, 32 and 128 krill m^{-2}. The addition of krill resulted in some negative values for fish abundance and hence biomass, as the level of predicted backscatter was lower than the backscatter 64 krill m^{-2} would have produced. To prevent negative down weighting of biomass estimates, all negative values for fish abundance were set to zero prior to calculating summary statistics for fish abundance and biomass. See table S11 for krill sensitivity analysis results.

Primary production required to support biomass

To assess whether the ecosystem could support such high levels of fish biomass, we estimated the amount of primary production (*P*, tonnes km^{-2} year^{-1}) required to support 570 Mt of mesopelagic fish biomass across the area modelled (*A*, 29,515,433 km^2). To estimate fish requirements we used equation S21 from [27], with slight modifications to annotation. Where biomass (*B,* tonnes km^{-2}), *t* is trophic level, which we assume to be 4.0 based on the trophic level of *E. antarctica* in [28], temperature (θ, °C) has been set at a mean value of 2.5°C for the study area modelled. We estimated krill requirements using the generic marine taxa equation S22 [27], assuming a trophic level of 2.5 for Antarctic krill [28], and biomass of 379 Mt (*A*,19 x 10^6 km^2) [29].

$$P = \left(\frac{B}{A}\right) \times 2.31t^{-1.72} \times exp^{0.053\times\theta} \qquad \text{Eq. S21}$$

$$P = \left(\frac{B}{A}\right) \times 20.19t^{-3.26} \times exp^{0.041\times\theta} \qquad \text{Eq. S22}$$

Resulting in a primary production requirement of 6.9 g C m^{-2} a^{-1} for mesopelagic fish and 22.5 g C m^{-2} a^{-1} for Antarctic krill. While challenging to quantify, the annual primary production for the pelagic regions of the Southern Ocean has been estimated at 54 g C m^{-2}a^{-1} [30], which is likely sufficient to support our estimate of fish biomass.

Supplementary Figures

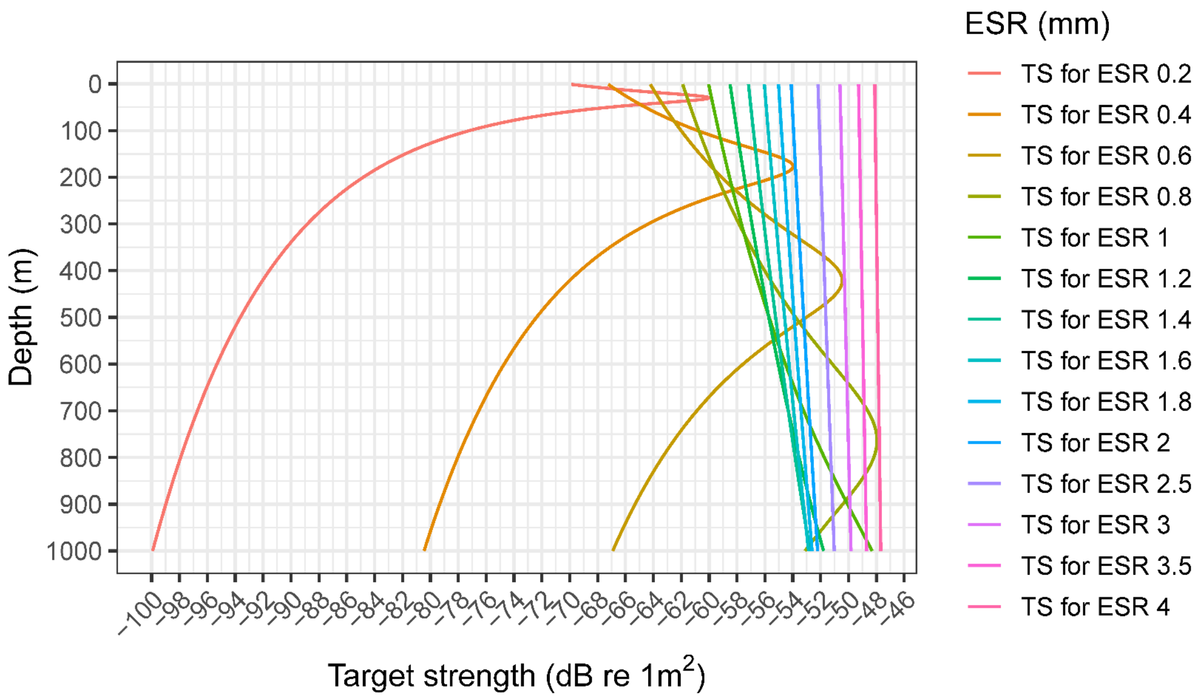

Figure S1. Frequency response plot for fish with theoretical range of swimbladder gas volumes at 38 kHz, modelled using prolate spheroid model [4-6]. Equivalent spherical radius (ESR) in mm. Model has fixed parameters of fish density at 1.054 g ml^{-1} (the mean density for gas-bearing fish species from this study) and prolate spheroid roundness of 0.3 (the average for *Krefftichthys anderssoni* measured from computed tomography scans, n = 4).

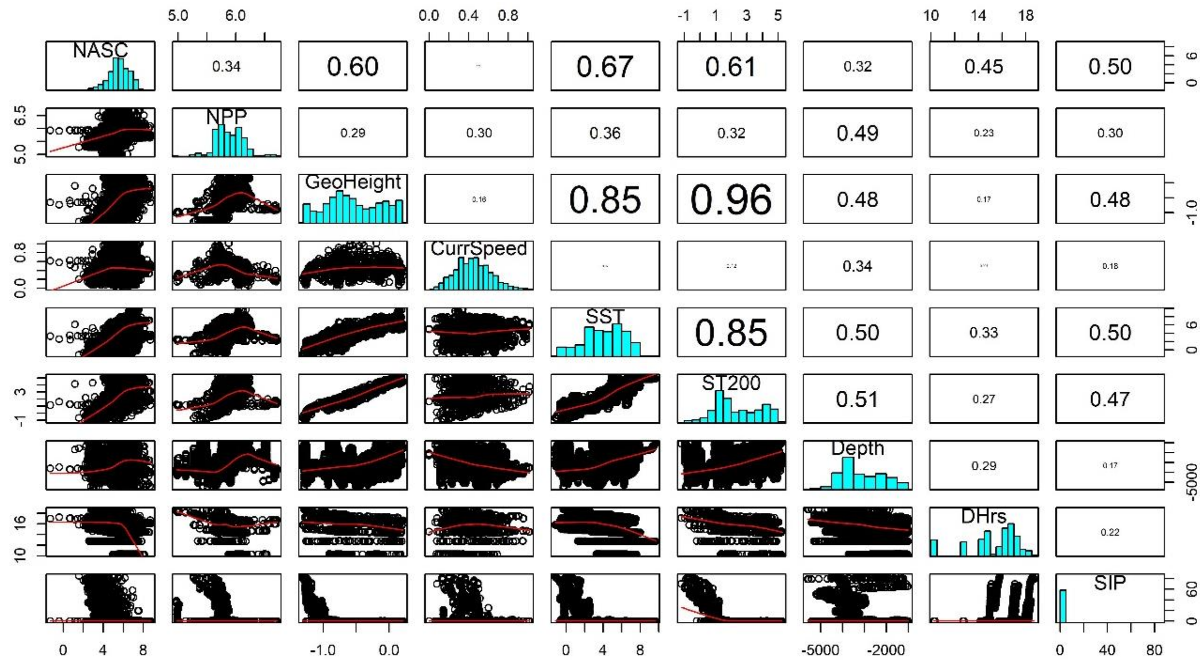

Figure S2. Pairplot of response variable $\log_e$ NASC (Nautical Area Scattering Coefficient, m^2 nmi^{-2}) and candidate environmental variables to assess for collinearity. Upper panel contains estimated pairwise correlations, size of font is proportional to absolute value of estimated Pearson correlation coefficients. Lower panel contains scatter plots with LOESS smoother. Diagonal panel contains frequency histograms for data visualisation.

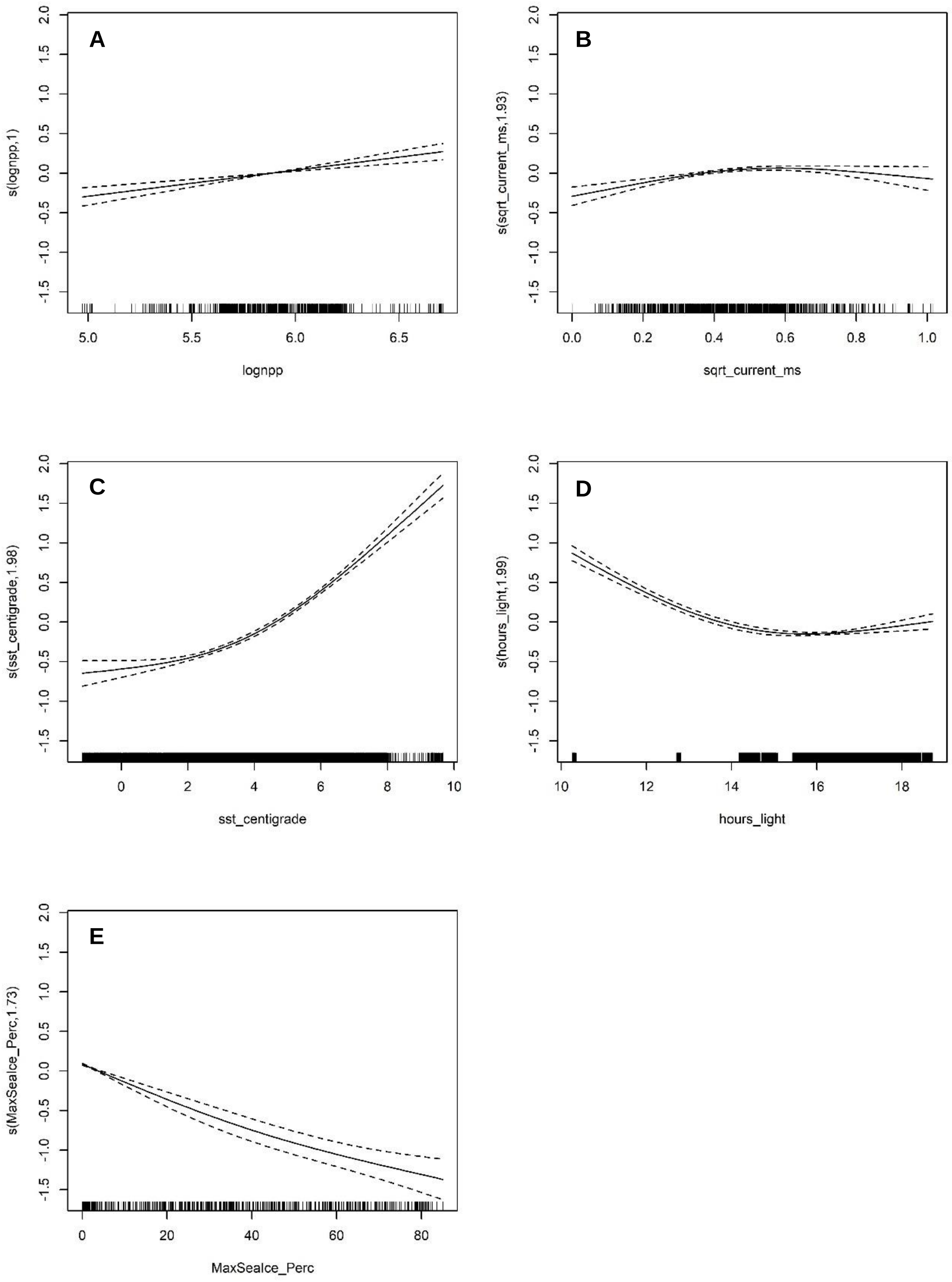

Figure S3. Estimated smoothing curves for the GAMM fitted to $\log_e$ Nautical Area Scattering Coefficient (NASC, m^2 nmi^{-2}) (a) $\log_e$ net primary productivity, (b) square root of geostrophic current speed, (c) sea surface temperature, (d) daylight hours, and (e) maximum percentage of sea ice. Dotted lines are ± 2 standard errors. Degrees of freedom in parenthesis. Rug plots on x-axis indicate number and distribution of observations.

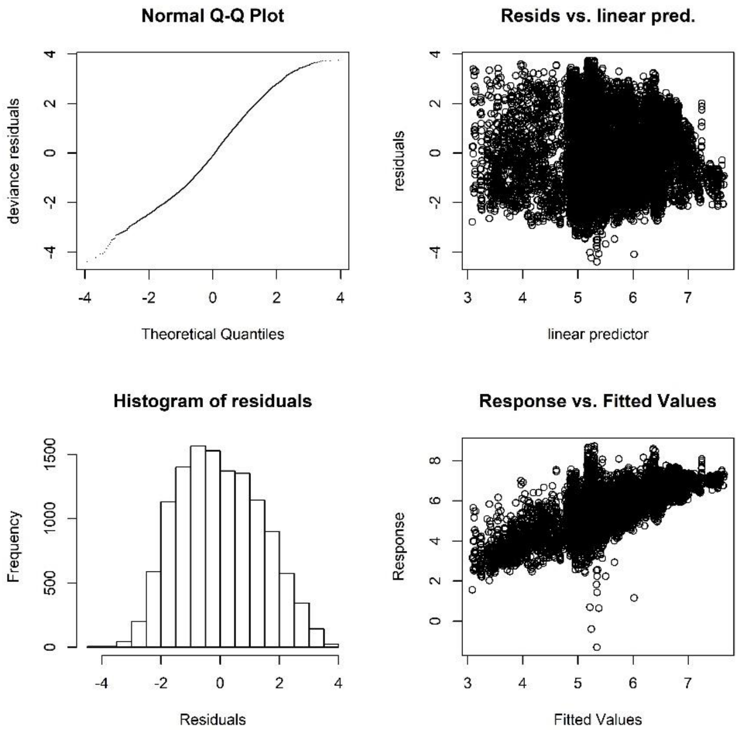

Figure S4. Model checking plots of final GAMM. Plots reveal some outlying residuals. However, the model is deemed acceptable, as whilst the model may occasionally over predict backscatter the vast majority of the residuals conform to normality.

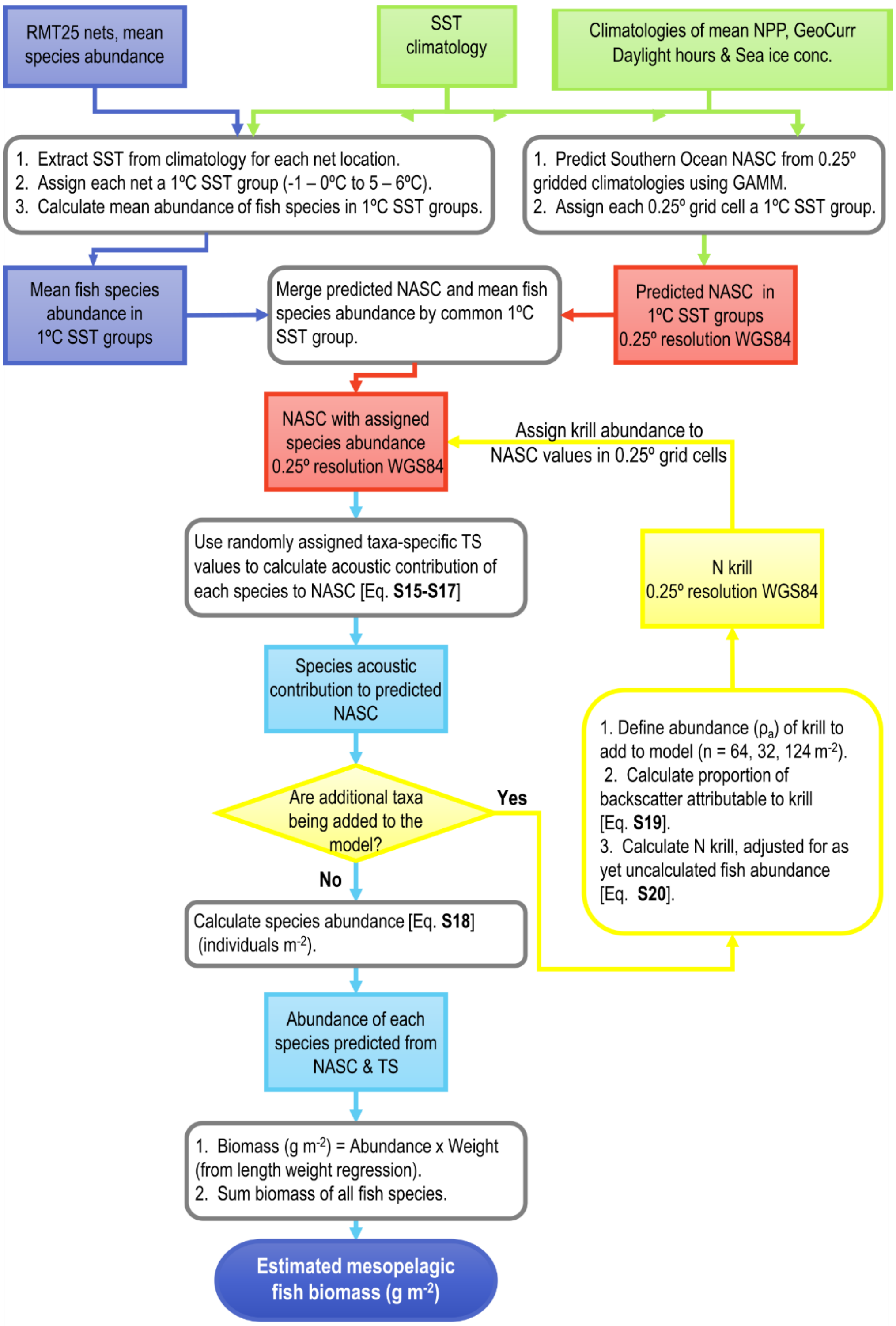

Figure S5. Data processing flow to calculate estimated mesopelagic fish biomass from raw RMT25 night, surface – 1000 m net data and environmental climatologies. SST: mean sea surface temperature Oct-Apr 2005-2017 [13], NPP: mean net primary productivity [14], GeoCurr: mean geostrophic current speed [15-17], mean daylight hours Oct-Apr [18], Sea ice conc.: mean sea ice concentration Sept only 2005-2017 [19]. Filled rectangles = data sets, unfilled rounded rectangles = processing step.

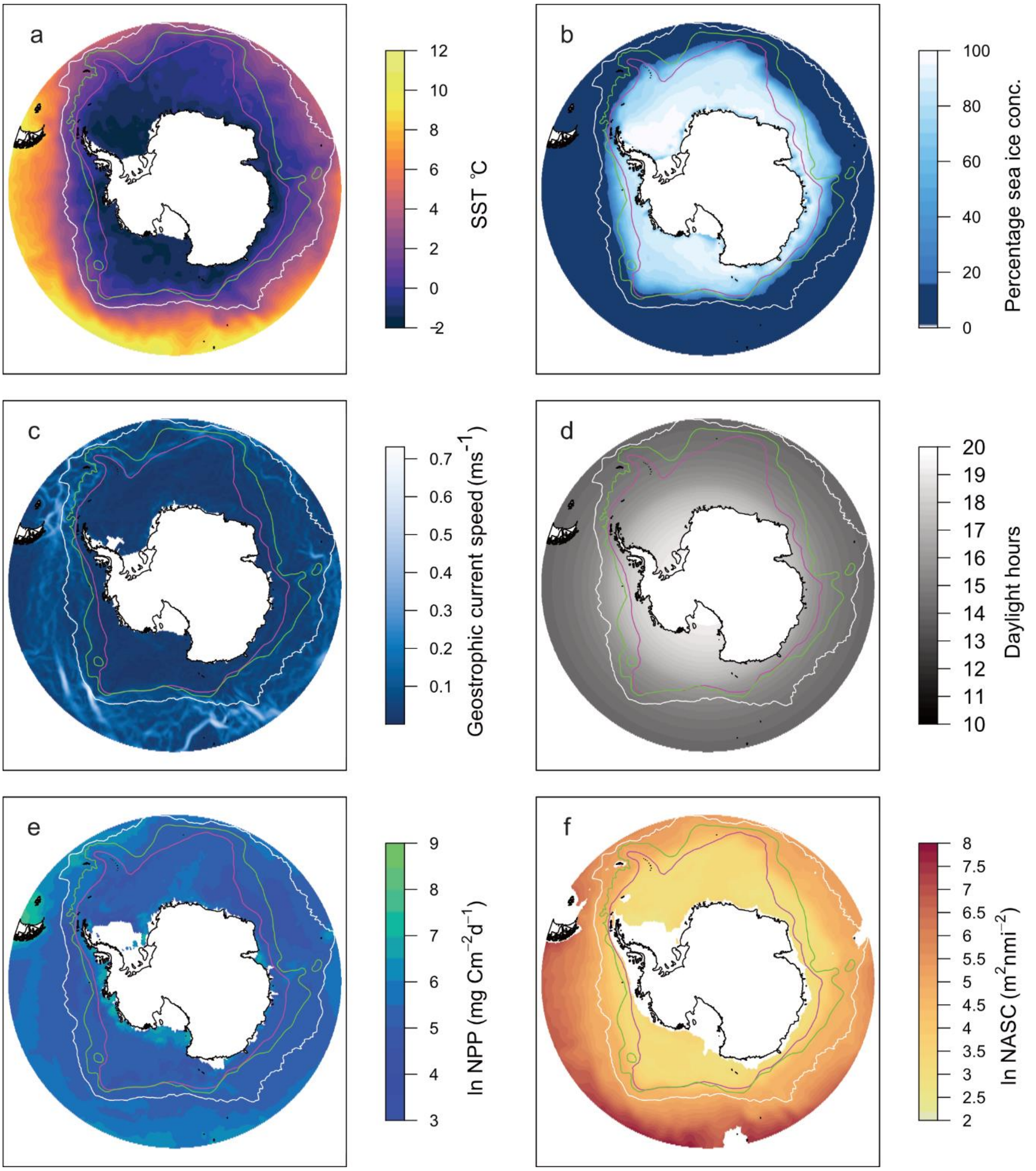

Figure S6. Southern Ocean variable plots with mean front positons. (a) Sea surface temperature climatology (Oct-Apr 2005-2017) [13], (b) Sea ice concentration climatology (Sep 2005-2017) [19], (c) Geostrophic current speed [15-17], (d) mean daylight hours (Oct-Apr) [18], (e) Net primary productivity ($\log_e$ mg C m^{-2} d^{-1}) [14], and (f) Predicted acoustic backscatter ($\log_e$ NASC). White regions indicate no data. Fronts: from north to south, Antarctic Polar Front (white), Southern Antarctic Circumpolar Current Front (green) and Southern Boundary (magenta).

Supplementary Tables

Table S1. Spatio-temporal summary of acoustic transect data used in generalised additive mixed model of NASC (Nautical Area Scattering Coefficient, m^2 nmi^{-2}). Transect date format year-month-day, and time is hours:minutes:seconds in GMT. Latitude (lat) and longitude (lon) both in decimal degrees South. Depth (m) – maximum depth of acoustic data.

Cruise leg ID	Start date (Y-M-D)	Start time (GMT)	End date (Y-M-D)	End time (GMT)	Start lat °S	Start lon °S	End lat °S	End lon °S	Depth (m)
JR16003_PF	2017-01-01	09:22:50	2017-01-08	23:59:58	55.30	41.36	60.36	60.67	1000
JR15004_002	2016-02-18	03:53:12	2016-02-20	22:20:25	60.31	46.78	52.81	57.09	1000
JR15004_001	2016-01-22	00:17:06	2016-01-24	11:05:19	52.45	56.65	60.42	45.17	1000
JR15002_007	2015-12-11	00:04:19	2015-12-14	00:09:42	52.63	39.12	51.74	56.11	1000
JR15002_001	2015-11-13	13:38:50	2015-11-15	12:33:18	53.55	55.33	60.30	46.82	1000
JR200_012	2009-04-15	23:49:39	2009-04-18	10:37:05	53.69	38.81	51.83	56.12	990
JR200_002	2009-03-13	22:20:14	2009-03-14	18:01:57	57.72	50.36	60.37	48.29	990
JR200_001	2009-03-12	02:22:40	2009-03-13	10:17:04	52.49	56.72	57.64	50.50	990
JR177_011	2008-02-14	07:26:11	2008-02-17	00:50:06	53.67	38.52	51.82	56.16	1000
JR177_001	2008-01-01	07:22:46	2008-01-03	17:38:28	53.53	55.55	60.29	47.65	1000
JR161_009	2006-11-30	16:44:51	2006-12-03	03:46:37	49.99	38.53	51.37	55.77	1000
JR161_002	2006-10-31	04:30:56	2006-10-31	18:56:32	58.02	50.25	60.47	49.10	800
JR161_001	2006-10-25	01:52:41	2006-10-27	00:19:08	52.58	56.86	57.62	50.49	800

Table S2. Overview of fish taxa included in mesopelagic fish biomass assessment and the morphological parameters assessed for Target Strength modelling. Swimbladder gas status as applied from literature. Current study: ✓ indicates new data collected and/or analysed during this study's assessment of fish acoustic properties, 'Est.' indicates that value was estimated from current study data, 'Lit.' indicates value was derived from literature. Where ρ_f is fish tissue density, LW_{reg} is Length-Weight regression, LW_{rat} is Length-Width ratio, TS is target strength model.

Family	**Taxon**	**Code**	**Swimbladder gas**	**Current study**			
				$\boldsymbol{\rho_f}$	**LW_{reg}**	**LW_{rat}**	**TS**
Myctophidae	*Electrona antarctica*	ELN	< 51.378 mm – Gas [1] ≥ 51.378 mm – No gas [1]	✓	✓	✓	✓
	Electrona carlsbergi	ELC	Gas [1]	✓	✓	✓	✓
	Gymnoscopelus braueri	GYR	Regressed – No gas [1]	✓	✓	✓	✓
	Gymnoscopelus fraseri	GYF	Regressed – No gas [1]	✓	✓	✓	✓
	Gymnoscopelus nicholsi	GYN	Regressed – No gas [1]	Est.	✓	✓	✓
	Protomyctophum bolini	PRM	Gas [1]	✓	✓	✓	✓
	Protomyctophum tenisoni	PRE	Gas [31]	Est.	✓	✓	✓
	Krefftichthys anderssoni	KRA	Gas [1]	✓	✓	✓	✓
Bathylagidae	*Bathylagus* spp.	BAX	No swimbladder – No gas [31]	✓	✓	✓	✓
Gonostomatidae	*Cyclothone* spp.	YTX	Fat invested – No gas [31]	Est.	✓	Est.	✓
Paralepididae	*Notolepis* spp.	NOE	No swimbladder – No gas [32]	Est.	Lit.	Est.	✓

Table S3. Densities measured during JR16003 (08 Dec 2016 – 19 Jan 2017) using modified density bottle method. ρ_f is density of fish tissue (g ml^{-1}), EGV is equivalent gas volume (mm^3) required to make fish neutrally buoyant in surrounding sea water at atmospheric pressure (see CTD cast number and CTD table S4 for sea water values), ESR equivalent spherical radius (mm) of gas volume, PGV percentage gas volume of fish. Gas values in 'red' are hypothetical as individuals are non-gas bearing species or size classes. All net types are remotely operated, multi net opening and closing systems: Rectangular Mid-water Trawls RMT25 and RMT8 have apertures (mesh sizes) of 25 m^2 (8–4.5 mm) and 8 m^2 (4.5–2.5 mm) respectively. MOCNESS is a Multiple Opening/Closing Net Sampling System with aperture 1 m^2 (mesh size 300 μm).

Species	SL mm	WW g	ρ_f g ml^{-1}	EGV mm^3	ESR mm	PGV %	Net event	Net no.	Net type	CTD cast
KRA	40	0.8	1.0374	7.596	1.219	0.975	146	2	RMT25	20
KRA	42	0.9	1.0394	10.214	1.346	1.166	143	2	MOCNESS	20
KRA	45	1.2	1.0342	7.760	1.228	0.664	146	2	RMT25	20
KRA	45	1.0	1.0394	11.349	1.394	1.166	146	2	RMT25	20
KRA	48	1.1	1.0394	12.484	1.439	1.166	147	1	RMT25	20
KRA	48	1.1	1.0374	10.445	1.356	0.975	147	1	RMT25	20
KRA	48	1.2	1.0357	9.452	1.312	0.809	147	1	RMT25	20
KRA	48	1.2	1.0309	4.264	1.006	0.365	164	2	RMT25	21
KRA	49	1.3	1.0374	12.344	1.434	0.975	147	1	RMT25	20
KRA	51	1.4	1.0372	12.983	1.458	0.953	146	2	RMT25	20
KRA	52	1.6	1.0394	18.159	1.631	1.166	146	2	RMT25	20
KRA	58	2.0	1.0447	32.632	1.982	1.676	171	1	RMT25	21
KRA	62	2.9	1.0447	46.930	2.238	1.662	146	1	RMT25	20
KRA	64	2.6	1.0427	37.333	2.073	1.475	146	1	RMT25	20
KRA	64	3.1	1.0374	29.849	1.924	0.989	171	1	RMT25	21
KRA	65	3.1	1.0342	20.461	1.697	0.678	171	1	RMT25	21
KRA	67	3.2	1.0427	46.376	2.229	1.489	171	1	RMT25	21
KRA	68	3.8	1.0364	32.549	1.981	0.880	146	1	RMT25	20
PRM	29	0.2	1.0619	6.295	1.145	3.234	89	1	MOCNESS	10
PRM	32	0.4	1.0735	16.808	1.589	4.316	164	2	RMT25	21
PRM	37	0.6	1.0757	26.365	1.846	4.514	164	2	RMT25	21
PRM	50	1.7	1.0656	59.715	2.425	3.608	164	2	RMT25	21
PRM	51	1.5	1.0686	56.057	2.374	3.840	39	2	RMT8	2
PRM	51	1.7	1.0619	54.161	2.347	3.273	164	2	RMT25	21
PRM	53	1.9	1.0637	62.888	2.467	3.401	129	2	RMT25	16
PRM	54	1.9	1.0619	60.533	2.436	3.273	164	2	RMT25	21
PRM	56	2.4	1.0568	65.073	2.495	2.785	147	2	RMT25	20
PRM	57	2.5	1.0568	67.398	2.525	2.770	129	2	RMT25	16
PRM	57	2.5	1.0568	67.784	2.529	2.785	147	2	RMT25	20
PRM	59	2.5	1.0607	76.585	2.634	3.147	147	2	RMT25	20
PRM	60	2.7	1.0607	82.294	2.698	3.132	129	2	RMT25	16
PRM	60	2.7	1.0540	66.635	2.515	2.535	147	2	RMT25	20
PRM	61	2.6	1.0540	63.765	2.478	2.520	129	2	RMT25	16
PRM	62	3.1	1.0540	76.027	2.628	2.520	129	2	RMT25	16
ELC	72	5.2	1.0568	140.187	3.223	2.770	129	2	RMT25	16
ELC	76	5.8	1.0619	183.114	3.523	3.244	129	2	RMT25	16
ELC	77	6.2	1.0568	167.146	3.417	2.770	129	2	RMT25	16
ELC	78	6.2	1.0671	224.029	3.768	3.713	129	2	RMT25	16
ELC	79	6.7	1.0607	204.212	3.653	3.132	129	2	RMT25	16

ELC	79	6.3	1.0632	205.986	3.664	3.359	129	2	RMT25	16
ELC	80	6.8	1.0637	225.072	3.774	3.401	129	2	RMT25	16
ELN	27	0.3	1.0553	7.743	1.227	2.651	143	1	MOCNESS	20
ELN	41	0.6	1.0394	6.890	1.180	1.179	171	1	RMT25	21
ELN	42	0.9	1.0394	10.334	1.351	1.179	171	1	RMT25	21
ELN	44	0.9	1.0342	5.623	1.103	0.642	39	2	RMT8	2
ELN	65	3.3	1.0342	20.831	1.707	0.649	129	2	RMT25	16
ELN	95	10.2	1.0254	-19.746		-0.199	129	2	RMT25	16
GYR	32	0.2	1.0247	-0.471		-0.242	171	1	RMT25	21
GYR	40	0.3	1.0247	-0.706		-0.242	171	1	RMT25	21
GYR	43	0.4	1.0394	4.593	1.031	1.179	171	1	RMT25	21
GYR	44	0.5	1.0262	-0.464		-0.095	171	1	RMT25	21
GYR	45	0.6	1.0309	1.959	0.776	0.335	129	2	RMT25	16
GYR	49	0.6	1.0342	3.787	0.967	0.649	129	2	RMT25	16
GYR	49	0.7	1.0342	4.620	1.033	0.678	171	1	RMT25	21
GYR	50	0.7	1.0309	2.286	0.817	0.335	129	2	RMT25	16
GYR	51	0.8	1.0309	2.612	0.854	0.335	129	2	RMT25	16
GYR	54	0.9	1.0342	5.940	1.124	0.678	171	1	RMT25	21
GYR	61	1.4	1.0292	2.274	0.816	0.167	129	2	RMT25	16
GYR	68	2.1	1.0277	1.021	0.625	0.050	164	2	RMT25	21
GYR	83	3.6	1.0277	0.715	0.555	0.020	129	1	RMT25	16
GYR	97	7.2	1.0247	-19.025		-0.271	129	1	RMT25	16
GYR	99	6.0	1.0277	1.191	0.658	0.020	129	1	RMT25	16
GYR	105	9.4	1.0247	-23.385		-0.256	146	2	RMT25	20
GYR	114	11.1	1.0254	-21.489		-0.199	129	1	RMT25	16
GYR	118	11.3	1.0247	-29.858		-0.271	129	1	RMT25	16
GYR	129	15.8	1.0277	5.578	1.100	0.036	147	1	RMT25	20
GYF	75	3.71	1.0686	139.955	3.221	3.875	164	2	RMT25	21
GYF	76	3.93	1.0582	112.162	2.992	2.932	164	2	RMT25	21
GYF	86	5.53	1.0656	194.249	3.593	3.608	164	2	RMT25	21
BAX	44	0.4	1.0595	11.721	1.409	3.011	112	1	RMT25	12
BAX	50	0.8	1.0477	15.138	1.535	1.944	146	2	RMT25	20
BAX	65	1.7	1.0394	19.294	1.664	1.166	146	2	RMT25	20
BAX	79	3.5	1.0374	32.417	1.978	0.952	112	1	RMT25	12
BAX	113	12.3	1.0342	76.675	2.635	0.641	112	1	RMT25	12
BAX	114	14.0	1.0309	44.610	2.200	0.327	112	1	RMT25	12
BAX	116	13.9	1.0374	131.984	3.158	0.975	143	1	MOCNESS	20
BAX	118	9.6	1.0374	88.915	2.769	0.952	112	1	RMT25	12
BAX	131	27.0	1.0309	92.331	2.804	0.351	146	2	RMT25	20
BAX	143	40.2	1.0309	137.470	3.202	0.351	146	2	RMT25	20
BAX	144	31.3	1.0309	99.736	2.877	0.327	112	1	RMT25	12
BAX	154	40.0	1.0277	4.794	1.046	0.012	112	1	RMT25	12

Table S4. Summary of oceanographic data collected by Conductivity Temperature Depth profiler during cruise JR16003 for use in fish gas volume calculations. Mean values were calculated from total water column (TWC). The mean of all six CTD cast seawater density at atmospheric pressure and sound speed values were used in fish Target Strength modelling.

CTD cast	CTD latitude	CTD longitude	Mean density of seawater (g ml^{-1})	Mean in-situ temperature (°C)	Mean sound speed (ms^{-1})
12	-55.24859	-41.26209	1.027565	1.707793	1464.151
16	-54.53799	-45.09371	1.027482	1.722665	1464.039
20	-53.90491	-49.27398	1.027319	2.673288	1468.015
21	-53.29432	-52.18519	1.027178	3.283250	1470.462
10	-52.80868	-40.11375	1.027584	1.783169	1464.472
2	-53.49266	-39.25101	1.027550	1.673574	1463.875

Table S5. Summary of net sample locations used to collect fish samples and estimate relative abundance. RMT group – net code identifying the stratified RMT25 nets which taken together sample the total water column (1000 m to surface) in the same location, code format is cruise number, followed by event numbers i.e. cruise_event_event. Latitude and Longitude are the mean latitude and longitude respectively of net sample tow locations in decimal degrees. Sample regime indicates if the sample was taken in day or night. During JR16003 a non-stratified sample 'TWC night' sampled the total water column, towed open from surface - 1000 m - surface, and was the source of samples for tissue density experiments and length frequency distribution only. 'PWC night' sampled the partial water column (400 m - surface), and was the source of samples for tissue density experiment only. Date – start date of the combined net sample.

RMT group	Latitude	Longitude	Sample regime	Date
JR16003_129_130	-54.62316	-45.15590	Night	2017-01-03
JR16003_146_147	-53.94665	-49.22128	Night	2017-01-04
JR16003_163_164	-53.27934	-52.18621	Night	2017-01-06
JR16003_112	-55.26142	-41.25934	TWC night	2016-12-31
JR16003_171	-56.71931	-56.85779	PWC night	2017-01-08
JR15004_60_61	-59.98448	-47.21586	Night	2016-02-02
JR15004_65_66	-60.00494	-46.62482	Night	2016-02-03
JR15004_72_73	-60.11098	-46.07252	Night	2016-02-04
JR15004_91_96	-60.29788	-46.44657	Night	2016-02-09
JR200_17_18	-60.47902	-48.35652	Night	2009-03-16
JR200_42_43	-60.26909	-44.28923	Night	2009-03-19
JR200_55_56	-59.72112	-44.11384	Night	2009-03-20
JR200_81_82	-58.02024	-42.93323	Night	2009-03-23
JR200_100_101	-58.01202	-43.09128	Night	2009-03-25
JR200_115_127	-56.78163	-42.26636	Night	2009-03-27
JR200_141_142	-55.23331	-41.37658	Night	2009-03-30
JR200_225_226	-50.04378	-33.74582	Night	2009-04-09
JR200_235_236	-50.59429	-33.78504	Night	2009-04-10
JR177_74_75_78	-60.54424	-48.27988	Day	2008-01-05
JR177_123_124	-60.19128	-44.64590	Night	2008-01-12
JR177_158_161	-59.69697	-44.09373	Night	2008-01-16
JR177_165_166	-59.68210	-44.09211	Day	2008-01-16
JR177_198_199	-58.01637	-43.04677	Night	2008-01-19
JR177_205_206_207	-58.02262	-43.05350	Day	2008-01-20
JR177_250_251	-55.21812	-41.27436	Day	2008-01-27
JR177_254_255	-55.21386	-41.25581	Night	2008-01-28
JR177_295_305	-52.86233	-40.07592	Night	2008-02-02
JR177_300_301	-52.87498	-40.14300	Day	2008-02-02
JR177_328_329	-52.73305	-39.01788	Night	2008-02-05
JR177_334_335	-52.63693	-39.09611	Day	2008-02-05
JR161_42_43_56	-57.59868	-50.51684	Night	2006-10-29
JR161_58_59	-57.72445	-50.42456	Day	2006-10-30
JR161_73_84	-60.50366	-48.87095	Night	2006-11-01
JR161_91_92	-60.59061	-49.03184	Day	2006-11-02
JR161_106_118	-60.45036	-44.59176	Night	2006-11-06
JR161_114_115	-60.44190	-44.55088	Day	2006-11-06
JR161_134_136	-59.57060	-44.25345	Night	2006-11-08
JR161_142_143	-59.54251	-44.26010	Day	2006-11-09
JR161_157_159	-57.32181	-42.75052	Night	2006-11-17
JR161_199_214	-55.24943	-41.27878	Night	2006-11-19
JR161_217_218	-55.29389	-41.36310	Day	2006-11-21
JR161_253_269	-52.98467	-40.35246	Night	2006-11-25
JR161_273_275	-50.09308	-38.11088	Night	2006-11-27
JR161_282_283	-49.98505	-38.09780	Day	2006-11-28

Table S6. Length-weight regression parameters calculated for key mesopelagic taxa. With the exception of *Notolepis* spp., frozen fish from RMT25 day and night net catches were weighed and SL measured to generate taxa specific length-weight regressions. Standard length (SL, mm) to biomass (wet weight, WW, g), WW = a SL^b. For *Notolepis* spp. (NOE) length-weight regression parameters were taken from FishBase (*Notolepis coatsi*). NOE SL was first converted to total length (TL, cm), using the conversion factor for the closely-related *Arctozenus risso* (fishbase.org) where fish total length (TL, cm), where TL = SL/10.65x10.

Species	**N**	**Min SL (mm)**	**Max SL (mm)**	**Mean SL (mm)**	**a**	**2.5% CI**	**97.5% CI**	**b**	**2.5% CI**	**97.5% CI**	**R^2**
BAX	11	44	154	105.0	4.43E-07	9.99E-08	1.96E-06	3.639	3.315	3.963	0.986
ELC	200	66	89	75.6	3.57E-05	1.42E-05	8.96E-05	2.787	2.574	3.000	0.771
ELN_L	1204	52	113	74.6	3.54E-06	3.05E-06	4.12E-06	3.291	3.256	3.326	0.966
ELN_S	180	24	51	45.1	6.51E-06	4.14E-06	1.02E-05	3.140	3.021	3.259	0.939
GYF	74	37	108	66.6	3.57E-06	1.98E-06	6.44E-06	3.253	3.112	3.393	0.967
GYN	51	33	166	126.2	4.42E-06	3.31E-06	5.90E-06	3.174	3.114	3.235	0.996
GYR	654	31	131	83.8	3.54E-06	2.95E-06	4.24E-06	3.180	3.138	3.221	0.972
KRA	517	24	70	46.2	6.23E-06	5.24E-06	7.41E-06	3.137	3.092	3.183	0.973
PRE	58	40	53	47.1	3.21E-05	8.80E-06	1.17E-04	2.744	2.408	3.080	0.827
PRM	315	21	63	46.2	1.20E-05	8.17E-06	1.78E-05	3.017	2.915	3.118	0.916
YTX	5	43	56	48.8	1.08E-06	7.31E-09	1.59E-04	3.309	2.023	4.595	0.957
NOE	-	-	-	-	0.00324	0.00123	0.00854	3.080	2.850	3.310	-

Table S7. Environmental variables considered for inclusion in assessment of environmental drivers of acoustic backscatter.

Variable	Abbreviation	Units	Resolution	Product
Sea surface temperature	SST	°C	0.01° grid Daily	GHRSST Level 4 MUR Global Foundation Sea Surface Temperature Analysis (v4.1) [33]
Sea temperature at 200m	ST_{200}	°C	0.25° grid Weekly	Copernicus Marine and Environment Monitoring Service (CMEMS) Products MULTIOBS_GLO_PHY_REP_015_002 [15-17]
Geopotential height (proxy for frontal positions)	GeoHeight	m		
Geostrophic current speed	CurrSpeed	m s^{-1}		
Net Primary Productivity	NPP	mg C m^{-2} d^{-1}	1/6° grid Jan-Mar 2005-2017 mean	Summer mean NPP for 2005-2017 generated by averaging monthly Jan-Mar NPP from the Ocean Productivity website (http://www.science. oregonstate.edu/ocean.productivity/index.php) [14]
Water depth (bathymetry)	Depth	m	30 arc-second grid intervals	GEBCO_2014 grid [34]
Maximum sea ice percentage cover	SIP	%	25 km grid Daily	National Snow and Ice Data Centre - Sea Ice Index, Version 3 [19]
Sea ice zone (ice conc. ≥15%)	SIZ	Presence /Absence		
Daylight hours	DHr	Hours	-	Calculated using R package 'geosphere' [18]
Day or Night	DN	Day /Night	-	Calculated using R package 'maptools' [35]

Table S8. Summary of GAMM fitting results. [NS]Not significant. DN – Day night, NPP – $\log_e$ net primary productivity (mg C m^{-2} d^{-1}), GeoCurr – square root geostrophic current speed (ms^{-1}), SST – sea surface temperature (°C), Depth – water depth (m), DHr – Daylight hours, SIP – max percentage sea ice (%). All GAMMs were specified as 'scaled t' family, with identity link function. Response variable $\log_e$ NASC. All explanatory variables were treated as smoothing terms (k = 3) with the exception of binomial term DN. While the full model had the lowest AIC, the final GAMM (outlined) was selected as it had a ΔAIC score <10, lowest BIC score and similar adjusted R^2 compared to the full model included smoothing terms for NPP, GeoCurr, SST, DHr and SIP.

Model	AIC	BIC	R^2 adj.	Scale est.	Test statistics of explanatory variables						
					t	F					
					DN	NPP	GeoCurr	SST	Depth	DHr	SIP
Full GAMM	16480.15	16598.85	0.583	1.197	2.08	34.04	11.70	316.89	8.67	153.66	97.40
Full GAMM – DN	16482.44	16593.72	0.582	1.199	NA	35.43	10.65	322.287	9.48	170.89	98.30
Full GAMM - NPP	16509.47	16613.33	0.575	1.217	2.38	NA	9.54	310.82	[NS]2.82	144.13	106.92
Full GAMM - GeoCurr	16492.30	16596.16	0.578	1.211	[NS]1.64	19.06	NA	322.19	12.89	144.44	104.92
Full GAMM - SST	16978.51	17082.37	0.446	1.598	3.00	16.72	14.75	NA	28.86	99.94	162.71
Full GAMM - Depth	16486.28	16590.14	0.580	1.204	2.28	26.36	16.13	349.55	NA	149.75	99.98
Full GAMM - DHr	16748.89	16852.75	0.516	1.391	5.153	13.41	1.74	254.91	3.62	NA	73.98
Full GAMM - SIP	16638.56	16742.42	0.544	1.307	[NS]1.76	49.37	18.50	681.72	10.20	122.83	NA
NPP only	17457.79	17494.88	0.149	2.443	NA	79.10	NA	NA	NA	NA	NA
GeoCurr only	17598.56	17635.66	0.003	2.875	NA	NA	[NS]2.52	NA	NA	NA	NA
SST only	16921.17	16958.27	0.450	1.578	NA	NA	NA	1250.0	NA	NA	NA
DHr only	17384.35	17421.45	0.206	2.281	NA	NA	NA	NA	NA	273.30	NA
SIP only	17313.45	17350.55	0.266	2.122	NA	NA	NA	NA	NA	NA	217.20
NPP GeoCurr SST DHr SIP	**16489.44**	**16585.88**	**0.579**	**1.207**	NA	27.17	14.82	353.01	NA	166.76	102.41
NPP SST DHr SIP	16506.34	16587.94	0.573	1.225	NA	13.98	NA	334.23	NA	153.17	118.13
SST DHr SIP	16523.27	16590.04	0.568	1.239	NA	NA	NA	374.10	NA	153.70	125.80

Table S9. Mean proportional abundance of fish taxa from RMT25 night-time total water column net samples, in 1 °C SST groups. Data were used to apportion predicted Southern Ocean NASC values among species in each 0.25° grid square. BAX – *Bathylagus* spp., ELC – *E. carlsbergi*, ELN L – *E. antarctica* (>51.378 mm), ELN S – *E. antarctica* (<51.378 mm), GYF - *G. fraseri*, GYN – *G. nicholsi*, GYR – *G. braueri*, KRA – *K. anderssoni*, NOE – *Notolepis* spp., PRE – *P. tenisoni*, PRM – *P. bolini*, YTX – *Cyclothone* spp.

SST	BAX	ELC	ELN L	ELN S	GYF	GYN	GYR	KRA	NOE	PRE	PRM	YTX
-1,0	0.2570	0.0000	0.4658	0.0471	0.0009	0.0050	0.1498	0.0000	0.0262	0.0000	0.0082	0.0400
0,1	0.2346	0.0000	0.4157	0.0403	0.0000	0.0221	0.2354	0.0015	0.0063	0.0000	0.0162	0.0279
1,2	0.1774	0.0678	0.1781	0.0475	0.0018	0.0081	0.2994	0.0948	0.0054	0.0100	0.0606	0.0490
2,3	0.0794	0.0732	0.1235	0.0275	0.0260	0.0134	0.1757	0.2005	0.0355	0.0233	0.1224	0.0995
3,4	0.0464	0.0326	0.0512	0.0166	0.0406	0.0228	0.2464	0.1859	0.0097	0.0589	0.1695	0.1195
4,5	0.0681	0.0038	0.0127	0.0066	0.0298	0.0084	0.1674	0.2120	0.0051	0.0378	0.2376	0.2107
5,6	0.0195	0.0000	0.0000	0.0074	0.0350	0.0498	0.0956	0.2632	0.0000	0.2681	0.1571	0.1043

Table S10. Sensitivity analysis results - varying fish standard length. Biomass (million metric tonnes) estimates are based on 2000 random permutations of fish standard lengths (TS) at median and interquartile range of fish standard lengths in the Scotia Sea and the Southern Ocean, assuming that fish are responsible for all of the acoustic backscatter.

Metric	All fish		Myctophidae only	
	Scotia Sea	Southern Ocean	Scotia Sea	Southern Ocean
Min.	11.77	232.96	9.09	176.49
1st. Qu.	15.67	310.96	12.11	234.98
Median	26.39	523.56	19.46	376.26
Mean	28.69	569.58	20.60	398.28
3rd. Qu.	41.10	819.48	28.14	546.20
Max.	61.89	1236.15	42.54	824.03
Variance	170.79	67449.98	71.97	26403.73
Std. Dev	13.07	259.71	8.48	162.49

Table S11. Sensitivity analysis results - krill included as source of backscatter. TS of fish randomly assigned based on the TS of fish at median fish standard length or interquartile range. 2000 random permutations of fish TS were applied (without replacement) for each of the krill abundance at rates of 64, 32 and 128 median sized krill m^{-2}. Biomass estimates are provided for all fish taxa and myctophid only.

Region (taxa)	ρ krill	Min.	1st. Qu.	Median	Mean	3rd. Qu.	Max.	Variance	Std. Dev
Scotia Sea (All fish)	64	6.68	9.32	15.55	16.96	24.16	35.15	58.8	7.67
	32	9.02	12.46	20.9	22.82	32.65	47.31	106.85	10.34
	128	4.31	6.01	10.1	11	15.61	22.82	24.69	4.97
Scotia Sea (Mycto)	64	5.3	7.42	11.91	12.66	17.36	25.34	27.63	5.26
	32	7.04	9.77	15.64	16.64	22.86	33.21	47.17	6.87
	128	3.48	4.88	7.91	8.42	11.52	16.94	12.43	3.53
Southern Ocean (All fish)	64	107.8	149.94	251.37	273.78	389.63	571.27	15361.8	123.94
	32	162.11	224.58	378.78	413.23	590.88	862.45	35268.4	187.8
	128	56.66	80.17	133.51	144.98	205.62	303.3	4266.61	65.32
Southern Ocean (Mycto)	64	84.66	118.22	189.22	201.04	274.25	404.26	6888.36	83
	32	124.78	173.39	277.83	294.4	403.04	588.94	14599.04	120.83
	128	45.73	64.61	104.09	110.55	150.97	224.28	2118.82	46.03

SI References

1. Dornan T, Fielding S, Saunders RA, Genner MJ. 2019 Swimbladder morphology masks Southern Ocean mesopelagic fish biomass. *Proc. R. Soc. Lond. B* **286**, 20190353. (doi:10.1098/rspb.2019.0353).
2. Stanton TK, Chu D, Wiebe PH, Clay CS. 1993 Average echoes from randomly oriented random-length finite cylinders: zooplankton models. *J. Acoust. Soc. Am*. **94**, 3463-3472. (doi:10.1121/1.407200).
3. Yasuma H, Takao Y, Sawada K, Miyashita K, Aoki I. 2006 Target strength of the lanternfish, Stenobrachius leucopsarus (family Myctophidae), a fish without an airbladder, measured in the Bering Sea. *ICES J. Mar. Sci.* **63**, 683-692. (doi:10.1016/j.icesjms.2005.02.016).
4. Andreeva IB. 1964 Scattering of sound by air bladders of fish in deep sound-scattering ocean layers. *Sov. Phys. Acoust.* **10**, 17-20.
5. Holliday DV. 1972 Resonance structure in echoes from schooled pelagic fish. *J. Acoust. Soc. Am.* **51**(4B), 1322-1332. (doi:10.1121/1.1912978).
6. Kloser RJ, Ryan T, Sakov P, Williams A, Koslow JA. 2002 Species identification in deep water using multiple acoustic frequencies. *Can. J. Fish. Aquat. Sci.* **59**, 1065-1077. (doi:10.1139/f02-076).
7. Hijmans RJ. 2018 raster: Geographic data analysis and modeling. (R package version 2.8-4 ed).
8. Zuur AF, Ieno EN, Elphick CS. 2010 A protocol for data exploration to avoid common statistical problems. *Methods Ecol. Evol.* **1**(1), 3-14. (doi:10.1111/j.2041-210X.2009.00001.x).
9. Wood S. 2019 mgcv: Mixed GAM computation vehicle with automatic smoothness estimation. (R package version 1.8-24 ed).
10. Legendre P. 1993 Spatial autocorrelation: trouble or new paradigm? *Ecology* **74**(6), 1659-1673. (doi:10.2307/1939924).
11. Paradis E, Schliep K. 2018 ape 5.0: an environment for modern phylogenetics and evolutionary analyses in R. *Bioinformatics* **35**(3), 526-528. (doi:10.1093/bioinformatics/bty633).
12. Pinheiro JC, Bates DM. 2000 *Mixed-Effects Models in S and S-PLUS*. New York, Springer.
13. Locarnini RA, Mishonov AV, Baranova OK, Boyer TP, Zweng MM, Garcia HE, Reagan JR, Seidov D, Weathers K, Paver CR, et al. 2018 World Ocean Atlas, Volume 1: Temperature. A. Mishonov Technical Ed. In *NOAA Atlas NESDIS 81* (pp. 1-52).
14. Behrenfeld MJ, Falkowski PG. 1997 Photosynthetic rates derived from satellite-based chlorophyll concentration. *Limnol. Oceanogr.* **42**, 1-20. (doi:10.4319/lo.1997.42.1.0001).
15. Guinehut S, Le Traon PY, Larnicol G, Philipps S. 2004 Combining Argo and remote-sensing data to estimate the ocean three-dimensional temperature fields - A first approach based on simulated observation. *J. Mar. Syst.* **46**(1-4), 85-98. (doi:10.1016/j.jmarsys.2003.11.022).
16. Guinehut S, Dhomps AL, Larnicol G, Le Traon PY. 2012 High resolution 3D temperature and salinity fields derived from in situ and satellite observations. *Ocean Sci.* **8**(5), 845–857. (doi:10.5194/os-8-845-2012).
17. Mulet S, Rio MH, Mignot A, Guinehut S, Morrow R. 2012 A new estimate of the global 3D geostrophic ocean circulation based on satellite data and in-situ measurements. *Deep-Sea Res. II* **77-80**, 70-81. (doi:10.1016/j.dsr2.2012.04.012).

18. Hijmans RJ. 2019 geosphere: Spherical Trigonometry. (R package version 1.5-10. ed).

19. Fetterer F, Knowles K, Meier W, Savoie M, Windnagel AK. 2017 Sea ice Index, Version 3. (Boulder, Colorado, USA, NSIDC: National Snow and Ice Data Center).

20. MacLennan DN, Fernandes PG, Dalen J. 2002 A consistent approach to definitions and symbols in fisheries acoustics. *ICES J. Mar. Sci.* **59**, 365–369. (doi:10.1006/jmsc.2001.1158).

21. Proud R, Handegard NO, Kloser RJ, Cox MJ, Brierley AS. 2018 From siphonophores to deep scattering layers: uncertainty ranges for the estimation of global mesopelagic fish biomass. *ICES J. Mar. Sci.* **76**(3), 718–733. (doi:10.1093/icesjms/fsy037).

22. Atkinson A, Hill SL, Pakhomov EA, Siegel V, Anadon R, Chiba S, Daly KL, Downie R, Fielding S, Fretwell P, et al. 2017 KRILLBASE: A circumpolar database of Antarctic krill and salp numerical densities, 1926–2016. *Earth Syst. Sci. Data* **9**(1), 193-210. (doi:10.5194/essd-9-193-2017).

23. Demer DA, Conti SG. 2005 New target-strength model indicates more krill in the Southern Ocean. *ICES J. Mar. Sci.* **62**, 25-32. (doi:10.1016/j.icesjms.2004.07.027).

24. McGehee DE, O'Driscoll RL, Traykovski LVM. 1998 Effects of orientation on acoustic scattering from Antarctic krill at 120 kHz. *Deep-Sea Res. II* **45**, 1273-1294. (doi:10.1016/S0967-0645(98)00036-8).

25. Fielding S, Watkins J, Cossio A, Reiss C, Watters G, Calise L, Skaret G, Takao Y, Zhao X, Agnew D, et al. 2011 The ASAM 2010 assessment of krill biomass for area 48 from the Scotia Sea CCAMLR 2000 synoptic survey. (Hobart, Australia, CCAMLR).

26. Atkinson A, Siegel V, Pakhomov E, Rothery P. 2004 Long-term decline in krill stock and increase in salps within the Southern Ocean. *Nature* **432**, 100-103. (doi:10.1038/nature02950).

27. Gascuel D, Morissette L, Palomares MLD, Christensen V. 2008 Trophic flow kinetics in marine ecosystems: Toward a theoretical approach to ecosystem functioning. *Ecol. Model.* **217**(1-2), 33-47. (doi:10.1016/j.ecolmodel.2008.05.012).

28. Stowasser G, Atkinson A, McGill RAR, Phillips RA, Collins MA, Pond DW. 2012 Food web dynamics in the Scotia Sea in summer: A stable isotope study. *Deep-Sea Res. II* **59**, 208-221. (doi:10.1016/j.dsr2.2011.08.004).

29. Atkinson A, Siegel V, Pakhomov EA, Jessopp MJ, Loeb V. 2009 A re-appraisal of the total biomass and annual production of Antarctic krill. *Deep-Sea Res. I* **56**(5), 727-740. (doi:10.1016/j.dsr.2008.12.007).

30. Arrigo KR, van Dijken GL, Bushinsky S. 2008 Primary production in the Southern Ocean, 1997–2006. *J. Geophys. Res. Oceans* **113**, C08004. (doi:10.1029/2007JC004551).

31. Marshall NB. 1960 Swimbladder structure of deep-sea fishes in relation to their systematics and biology. *Discovery Reports* **31**, 1-122.

32. Post A. 1990 Paralepididae. In *Fishes of the Southern Ocean* (eds. Gon O., Heemstra P.C.), pp. 138-141. (Grahamstown, South Africa, J.L.B. Smith Institute of Ichthyology).

33. JPL MUR MEaSUREs Project. 2015 GHRSST Level 4 MUR Global Foundation Sea Surface Temperature Analysis (v4.1). (California, USA, PO.DAAC).

34. GEBCO. 2014 The GEBCO_2014 Grid.

35. Bivand R, Lewin-Koh N. 2018 maptools: Tools for handling spatial objects. (R package version 0.9-4 ed).